Astron. Astrophys. 347, 1039–1045 (1999)

ASTRONOMY AND ASTROPHYSICS

Jupiter's magnetic field as revealed by the synchrotron radiation belts

II. Change of the 2-D brightness distribution with D_E

G.A. Dulk[1], **Y. Leblanc**[1], **R.J. Sault**[2], **and S.J. Bolton**[3]

[1] CNRS–URA 264, Departement de Recherche Spatiale, Observatoire de Paris, F-92195 Meudon, France
[2] Australia Telescope National Facility, CSIRO, Epping, NSW 1710, Australia
[3] Jet Propulsion Laboratory, Pasadena, CA, USA

Received 29 March 1999 / Accepted 30 April 1999

Abstract. We analyze the magnetic equatorial component of Jupiter's radio synchrotron radiation belts using two-dimensional images recorded by the Australia Telescope Compact Array and the Very Large Array over a period of several years, during which D_E, the Earth's declination seen from Jupiter, changed from $D_E = -2.9°$ to near 0°. The brightness distribution of the belts changed markedly. When $D_E = -2.9°$ there is a pronounced east-west asymmetry where the brightness of a region traversing the east limb is markedly different from that of the same region traversing the west limb, 180° of rotation later. At most longitudes λ_{III} the brightness at east limb passage is larger than at west limb passage. However, when $D_E \approx 0°$, the east-west asymmetry essentially disappears. When $D_E = +2.9°$ it is predicted that the east-west asymmetry will be as at $-2.9°$, but reversed.

We show how these changes of appearance are simply related to D_E and the warp of Jupiter's field as described by the "magnetic declination". The radius, latitude and brightness of the locus of maximum intensity is determined by electrons of pitch angle $\alpha_{\rm eq} \approx 90°$, and its longitudinal variation depends entirely on the magnetic field of Jupiter, and not on the energy distribution of the relativistic electrons. We compare the observations with calculations from three magnetic field models and find them to be consistent in general but discrepant in detail. The differences are attributed to uncertainties in the field models, which were generated with few constraints coming from the low latitudes and small radii of the synchrotron radiation belts.

Key words: magnetic fields – plasmas – radiation mechanisms: non-thermal – planets and satellites: individual: Jupiter – radio continuum: solar system

1. Introduction

The radio synchrotron radiation from Jupiter, produced by relativistic electrons trapped in Jupiter's magnetic field, provides otherwise unobtainable information on the magnetic field and the energy and pitch angle distributions of the electrons. The radiation mechanism is well understood, but the magnetic field at small radii and low latitudes is not well determined, nor are the detailed properties of the electrons.

In Paper I (Dulk et al. 1999) we used a 3-D reconstruction of the radiation belts to derive some properties of the magnetic field. Certain aspects of these derived properties are not in accord with present models of the field, which is not surprising because past observations have provided few constraints at small radii and low latitudes. Future models of the field may benefit from the constraints provided by the synchrotron radiation.

In addition to tracing out Jupiter's magnetic field, our observations permit us to understand how changes in D_E, the declination of the Earth as seen from Jupiter, affects the longitude profile of the magnetic equatorial radiation. This is the subject of this Paper II.

Our observations span the changing D_E from approximately its maximum southerly value of $-2.9°$ in July 1995 to essentially 0° in May and November 1997. As shown by Leblanc et al. (1997) and Dulk et al. (1997), changes in D_E strongly affect Jupiter's appearance in a way that depends almost entirely on D_E and on the warp of the magnetic equator. This is because the synchrotron radiation is beamed in the direction of the relativistic electron motion, and that the major population of electrons with pitch angles $\alpha_{\rm E} \approx 90°$ emit most intensely perpendicular to the field, i.e. tangent to the local equatorial surface. Thus an observer as little as two or three degrees off this surface receives a lowered intensity. When $D_E \neq 0°$ the warp of the magnetic equatorial field produces a pronounced east-west asymmetry, where the brightness of a given location when it traverses the east limb differs from the brightness of the same location when it traverses the west limb, 180° of rotation later. The variation with longitude of this asymmetry depends only on the magnetic field and not on the energy or pitch angle distributions of the relativistic electrons. Hence the asymmetry provides a good diagnostic of the magnetic equatorial field at the small radii and low latitudes where the field strength is about 1.2 G.

In Sect. 2 we describe the observations, where we concentrate on the east-west asymmetry of the magnetic equatorial radiation, and its changes with D_E. We do not study the radiation from high latitudes on the planet which is due to electrons

Send offprint requests to: G.A. Dulk

with smaller pitch angles than are of concern here. In Sec. 3 we compare our observations with predictions of different magnetic field models and show that, while they account qualitatively for the observations, there are discrepancies that shed light on the inadequacies of the field models. Then in Sec. 4 we summarize and conclude.

2. Observations and imaging

We have four sets of observations between July 1995 and November 1997, measured using two different radio interferometers. Three observations were done with the Australia Telescope Compact Array (ATCA) at $\lambda = 22$ cm and one with the Very Large Array (VLA) at $\lambda = 20$ cm. During that time the jovicentric value of D_E changed from $-2.9°$ to $+0.03°$. Table 1 gives some of the relevant parameters.

Each of the three ATCA observations were made over ten days, with 11 to 12 hours per day, in two five-day sessions separated by a five-day gap. This observing scheme optimizes the Fourier plane coverage at many longitudes. This is needed because the ATCA, unlike the VLA, has limited instantaneous sampling of the Fourier plane (it is an east-west array), The VLA observations were made for about 8 hours per day on four days, 6, 7, 11, and 12 May, thus covering more than two complete Jovian rotations. All of the data sets are of excellent quality except that of November 1997 where the Fourier coverage was incomplete due, in part, to instrumental problems.

This paper is based on two-dimensional images constructed every 20° of central meridian longitude (CML) from data recorded at the given $CML \pm 20°$. A standard construction technique was used to ensure the images from the different epochs were directly comparable. After normal calibration, a 350 K black body disk (corresponding to Jupiter's thermal emission) and background confusing sources were subtracted from the data. The data were adjusted so the resultant images would represent Jupiter at a standard orientation and distance of 4.04 AU. We used standard radio interferometric imaging followed by maximum entropy deconvolution. The resulting images were then convolved to a consistent resolution of about 70% of the point-spread function width (i.e. the images are mildly super-resolved) and the residuals folded back in. Although all four Stokes parameters were measured, here we use only the images of total intensity, converted to brightness temperature.

2.1. Sample images showing the east-west asymmetry

Fig. 1 shows two images from the ATCA in 1995 when $D_E = -2.9°$ and two from the VLA in May 1997 when $D_E = -0.04°$. The two images of each pair were made from data separated by 180° of Jupiter rotation, i.e., $CML = 20°$ and 200°. The region on the east (i.e. left) limb when $CML = 20°$ is on the west (right) limb at 200°. CML is awkward to use because it is defined with respect to the observer, not with respect to longitudes on Jupiter. It is better to use λ_{III}, the system III longitude on Jupiter itself. To convert from CML to λ_{III}, we add 90° to the CML for east limb data and subtract 90° from

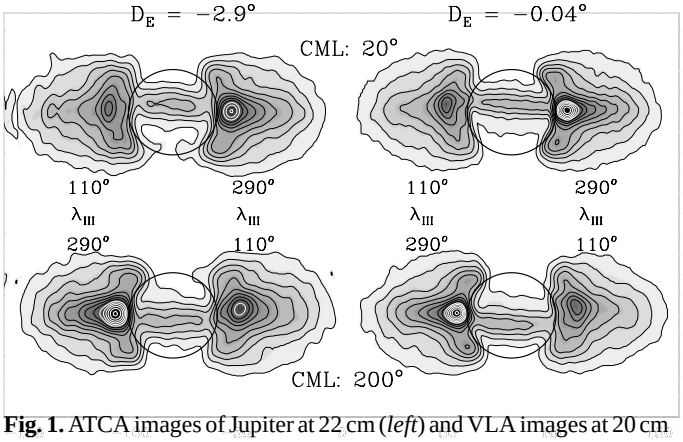

Fig. 1. ATCA images of Jupiter at 22 cm (*left*) and VLA images at 20 cm (*right*), at $CML = 20°$ (*top*) and 200° (*bottom*). The longitudes λ_{III} of regions traversing the limbs is indicated. Thermal radiation from the disk has been removed. The circle shows the disk of Jupiter. Black contours are at brightness temperatures 100 to 900 K and white contours are at 1000 K and above. The ATCA images when $D_E = -2.9°$ are NOT mirror images, as they would be if there were no east-west asymmetry. On the contrary, the VLA images at $D_E = -0.04°$ are close to being mirror images.

Table 1.

Date	Telescope	Jupiter's Declination	Restored Resolution	D_E
1995 July	ATCA	$-20.7°$	$8'' \times 3''$	$-2.9°$
1996 July	ATCA	$-22.9°$	$8'' \times 3''$	$-1.7°$
1997 May	VLA	$-15.3°$	$8'' \times 3''$	$-0.04°$
1997 Nov	ATCA	$-17.8°$	$20'' \times 6''$	$+0.03°$

west limb data. As seen in Fig. 1, the region at $\lambda_{III} = 110°$ is on the east limb when $CML = 20°$ and on the west limb when $CML = 200°$.

The 1995 ATCA images on the left, when $D_E = -2.9°$, show a distinct east-west asymmetry. For example, the brightness of the region at $\lambda_{III} = 290°$, on the west limb in the top image, is lower by about 300 K than it is on the east limb in the bottom image.

In contrast, the VLA images on the right, when D_E was nearly 0°, have almost no east-west asymmetry. The brightness at $\lambda_{III} = 290°$ is approximately the same on both the east and west limbs.

The radiation in front of the disk of Jupiter is visible in both the ATCA and VLA images. In the top images at $CML = 20°$ the northern end of the magnetic dipole is tilted away from the observer, so the equatorial radiation belt appears concentrated to the north of disk center. At $CML = 200°$ the northern end of the dipole is tilted toward the observer so the equatorial radiation is larger to the south of disk center.

The brightness temperature of the radiation in front of the disk is only about 400 K, i.e. much smaller than above the limbs. This "limb brightening" effect is due to the optical thickness being larger above the limbs. In particular the optical thickness is largest at limb passage of locations where the observer is located

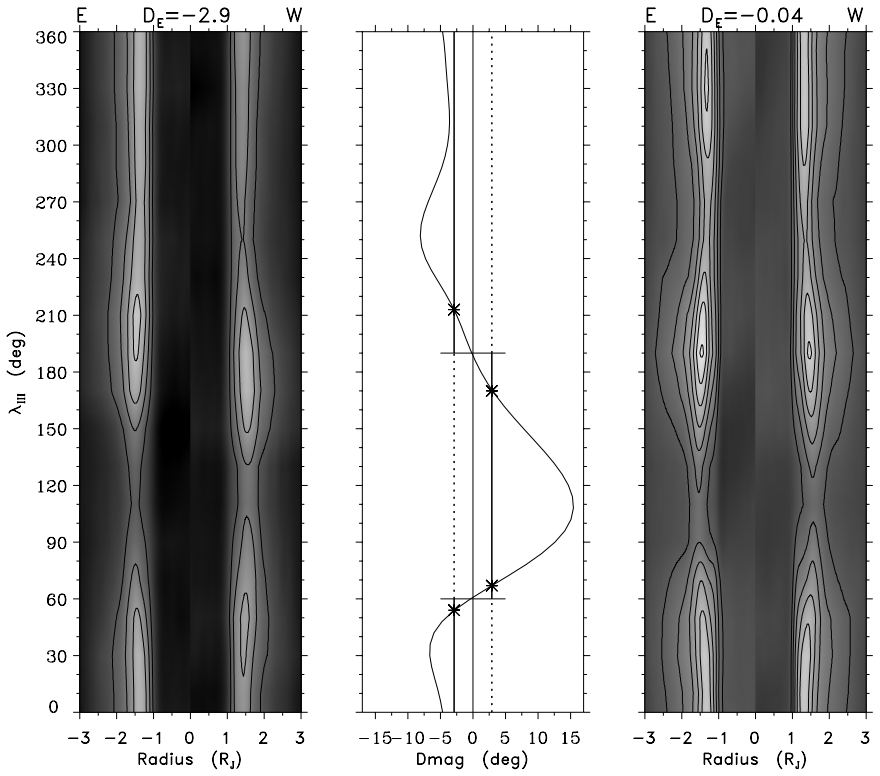

Fig. 2. Brightness vs. radius and Jovian longitude λ_{III} for ATCA observations at $D_E = -2.9^\circ$ (*left panel*) and VLA observations at $D_E = -0.04^\circ$ (*right panel*). The brightness profiles were taken from east to west along the magnetic dipole equator on images at 20° increments of CML. The east (west) halves of the profiles were converted to λ_{III} by adding (subtracting) 90° to the CMLs before plotting them here.

exactly in the plane tangent to the local magnetic equator. This phenomenon is discussed below in terms of D_E and the warp of the magnetic equator as described by the magnetic declination D_{mag}.

2.2. Brightness vs. λ_{III} in the dipole equator

We have images similar to those of Fig. 1 every 20° of CML, from which we have taken cuts along the "dipole equator". Here we define the "dipole equator" to be the magnetic equatorial plane of a dipolar approximation to the Jovian field. We take this dipole as having its north pole tilted from the rotation axis towards $\lambda_{III} = 200^\circ$ by 10°. Our objective is to compare brightnesses east vs. west as different Jovian longitudes λ_{III} traverse the limbs. To do this we have converted the east and west halves of the equatorial cuts from CML to λ_{III} and then have joined them in the middle. Fig. 2 shows the results. (Leblanc et al. (1997) showed a similar figure from ATCA observations at 13 cm, without the conversion from CML to λ_{III}.)

In the right panel, the VLA observations at $D_E = -0.04^\circ$, the brightness east and west of center is almost the same at all λ_{III}. In contrast, in the left panel, the ATCA observations at $D_E = -2.9^\circ$, there is a distinct east-west asymmetry: the brightness of most regions at east limb passage is larger than at west limb passage, and the peak brightness occurs at different longitudes on the two limb passages: $\lambda_{III} \approx 210^\circ$ and $\approx 180^\circ$ respectively.

The difference in the two sets of observations can be attributed solely to D_E, and we will now show how the asymmetries are related to D_E and the magnetic declination D_{mag}.

3. Brightness and the magnetic field

In this section we concentrate on understanding the brightness of the magnetic equatorial radiation and the character of the magnetic field.

3.1. Brightness and D_{mag} in the dipole equator

As noted by Dulk et al. (1997) and in Paper I, at each point around Jupiter's magnetic equator, the magnetic declination D_{mag} (the angle between the plane perpendicular to the field and the plane perpendicular to Jupiter's rotational axis) is

$$D_{mag} = \arctan(B_\phi / B_\theta), \tag{1}$$

where B_ϕ B_θ are the azimuthal and colatitudinal components of the field. The synchrotron radiation from relativistic electrons with pitch angles near 90° is concentrated in the plane perpendicular to the field, while the Earth is located in the plane perpendicular to the rotational axis when $D_E = 0^\circ$, and is 2.9° south of it when $D_E = -2.9^\circ$.

We have calculated the longitude profile of D_{mag} in three models of the magnetic field, O6, H4 and VIP4. In Paper I (Fig. 2) we compared these profiles at the locus in the magnetic equator where $B = 1.2$ G, and showed that the H4 model, while not perfect, is more consistent with the observations than are the other two; therefore we use it to illustrate the relationship between D_{mag} and brightness.

The middle panel of Fig. 2 shows D_{mag} calculated from the H4 model. When longitudes where D_{mag} is positive are on the east limb, the beam of magnetic equatorial radiation is centered northward of the Jovigraphic equator, and when they are on the

west limb the beam of radiation is centered southward of the Jovigraphic equator.

Most striking is near $\lambda_{III} = 110°$, the location of the large excursion of D_{mag} to its maximum value of $+15°$: little intensity is received at the Earth from that λ_{III}. The Earth would have to be 15° above or below Jupiter's equatorial plane to be directly in the beam of radiation.

When $D_E \approx 0°$, as in the right panel, the Earth is equally far from the beam at east and west limb passage of all longitudes, thus the east and west limb brightness profiles are nearly equal. In the middle panel of Fig. 2, $D_E = 0°$ corresponds to the Earth being along the central line, the zero of D_{mag}. Then it is the absolute value of D_{mag} that determines the brightness observed, the same on east and west. The general correlation of brightness and $|D_{mag}|$ is very good. The peak brightness occurs at $\lambda_{III} \approx 110°$, one of the two zero crossings of D_{mag}, a time when the Earth is directly in the beam. However, there is no similar peak at $\lambda_{III} \approx 60°$ when again the Earth is in the beam. This difference is attributable to the slopes at the two zero crossings, the slope being inversely proportional to the depth along the line of sight of the radiation beamed toward Earth, and hence inversely proportional to the optical depth and the brightness. As shown in Paper I, an improved magnetic field model would have a steeper slope at $\lambda_{III} = 60°$ than is in the H4 model, and much steeper than in the O6 or VIP4 models.

Now consider the left panel, where $D_E = -2.9°$. When the large excursion at $\lambda_{III} = 110°$ is on the east (west) limb, the Earth is 2.9° farther from (closer to) the beamed radiation. Thus the eastern brightness minimum is deeper than is the western brightness minimum. Noting that D_{mag} is negative everywhere from $\lambda_{III} = 190°$ to 60°, and in that range the beam of magnetic equatorial radiation is southward directed on east limb passage, we can understand why the east limb brightness is the larger.

In the middle panel of Fig. 2 the short horizontal lines mark the zero crossings of D_{mag} in the H4 model, and there are vertical lines at $\pm 2.9°$, partly solid and partly dotted. The line at $-2.9°$ ($+2.9°$) relates to east (west) limb brightness, and the distance of this line from the D_{mag} curve should be proportional to the brightness at east (west) limb passage. In general there is a very good proportionality between the two, for both limbs.

The distance between the curve D_{mag} and the vertical lines is the angle between the viewing direction and the direction of maximum intensity. For sources on the east and west limbs, the respective angles θ_E and θ_W are given by the relations:

$$\theta_E = |D_{mag} - D_E| \qquad \text{and} \qquad \theta_W = |D_{mag} + D_E| \,. \quad (2)$$

The solid portions of the vertical lines denote longitudes where the east (west) limb brightness should be the larger, and this is borne out. The stars mark the longitudes where $D_{mag} = D_E$, i.e. where the Earth is directly in the beam, and there should be a maximum of intensity. Indeed, the principal maxima of brightness are in the region near 190°, that of the east limb is near the predicted value of 210° and that of the west limb is near the predicted value of 170°. On the other hand, for the reason discussed above, the predicted maxima near 60° do not exist.

The comparison in Fig. 2 is a qualitative one because the brightness profiles come from the dipolar magnetic equator, while the D_{mag} curve relates to the warped magnetic equator. Nevertheless the figure shows graphically that the east and west limb brightness variations with longitude and their changes with D_E are well, but not perfectly explained by D_{mag} in the H4 model.

3.2. Brightness and D_{mag} in the true magnetic equator

In our series of two-dimensional images at varying CMLs, we have measured the maximum of intensity on both the east and west limbs. We now describe this maximum brightness and its changes with D_E.

In Fig. 3, the symbols show the brightness temperature measured at the maxima on the east limb (squares) and west limb (diamonds) for three sets of observations. In the top panel, $D_E = -2.9°$, the symbols for east and west limbs are well separated and the variation with λ_{III} is different at the two limbs. In the center panel $D_E = -1.7°$, the data for the east and west limbs are moderately separated and they vary with λ_{III} similarly. And in the bottom panel, $D_E = -0.04°$, the data for the east and west limbs are little separated and vary almost identically with λ_{III}.

The dashed and dot-dashed curves on Fig. 3 are calculations of θ_E and θ_W from Eqn. 2. They are consistent with the observations in their general form and in the fashion that they approach each other as D_E approaches zero.

The physical relationship between brightness temperature and D_{mag} is unknown, and so the same is true for θ_E and θ_W. Therefore for the curves of Fig. 3 we have adjusted the amplitude of θ_E in degrees (right scale) to match approximately the amplitude of the E limb brightness variation, and smoothed them to the $\pm 20°$ resolution of the observations in λ_{III}. We then used the same scaling for θ_W.

In Fig. 3 it is evident that the curves for θ_E and θ_W do not exactly reproduce the observations, particularly in the range of $\lambda_{III} \approx 330°$ to 50°. As in Paper I we attribute most of the differences to uncertainties in the H4 model. We have made a similar comparison using the O6 and VIP4 models, and in general the match with the observations is poorer. In particular, the bottom panel of Fig. 4 shows the same brightness data as in Fig. 3, but a comparison is made between the H4 and VIP4 models. At most longitudes, particularly from 60° to 110°, the H4 model provides the better fit.

3.3. Residual asymmetry at $D_E \approx 0$

As the assymetry depends on $|D_E|$, we expected that the May 1997 observations at the VLA when D_E was as only $-0.04°$ would show no asymmetry. However, the bottom panels of Fig. 3 and 4 show that a small asymmetry remains in the VLA observations, with the brightness at east limb passage being slightly but definitely larger than at west limb passage, particularly near $\lambda_{III} = 190°$. Similarly we expect no asymmetry from November 1997 observations at the ATCA when $D_E = +0.03°$. How-

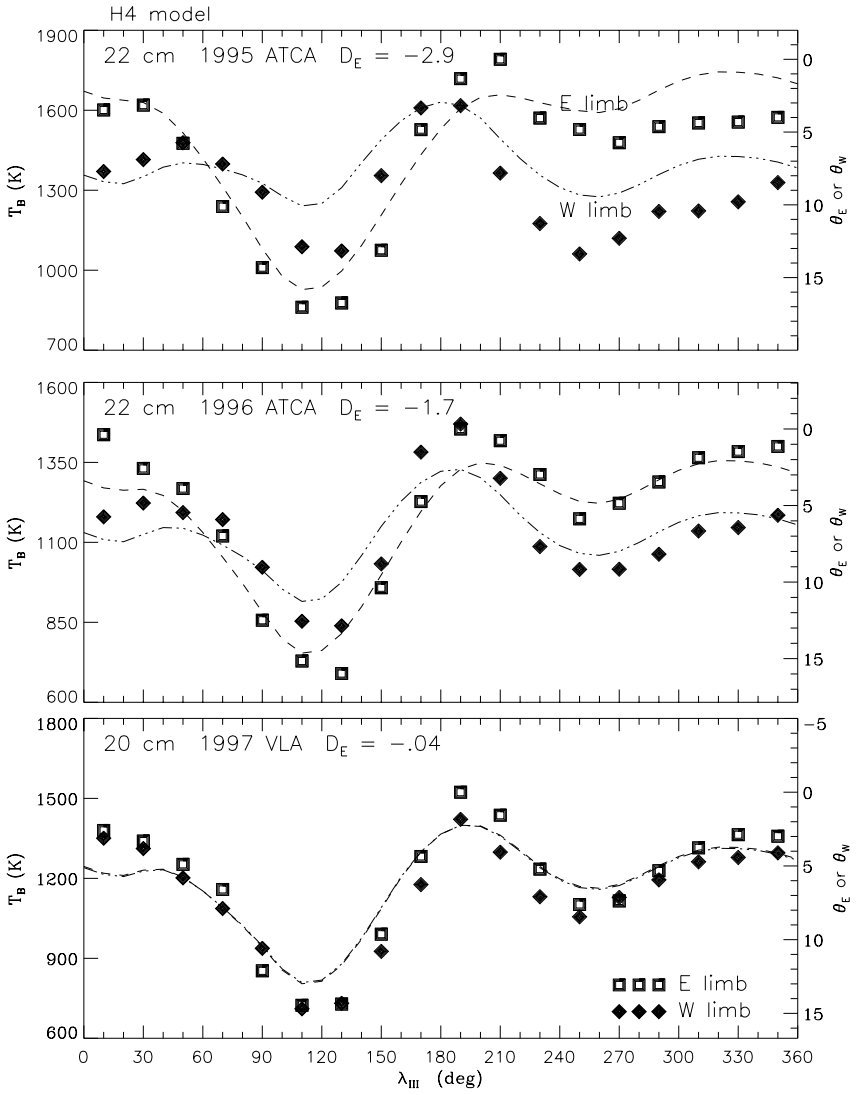

Fig. 3. The symbols show the maximum brightness temperature vs. λ_{III} (left scale) of the equatorial radiation as observed on the east limb (squares) and west limb (diamonds). The three panels correspond to observations at three values of D_E. The curves and the right scale show the angles from Eqn. 2 for the east limb (θ_E, dashed line) and west limb (θ_W, dash-dot line) as calculated from the H4 model. In the bottom panel, where $D_E = -0.04°$, the two curves are indistinguishable.

ever there is a similarly small asymmetry in the ATCA data, in the opposite sense to the VLA, at a level just above the noise.

There are several possible origins of this remaining asymmetry. 1) It is not real, but within the uncertainties of the observations. This seems not to be the case, at least for the VLA observations. We have estimated the level of the systematic errors by dividing the data into two independent sets. We find the asymmetry in both data sets at about the same level. 2) The asymmetry is real and is the result of the remaining, very small D_E of $-0.04°$ and $+0.03°$ of the two sets of observations. This seems improbable, and there is no substantiation of the idea in existing magnetic field models. 3) The asymmetry is real and is due to a dawn-dusk effect on Jupiter. The VLA observations of May 1997 were made near eastern quadrature, and therefore biased by about 11° toward the dusk side of Jupiter, with the east limb being in 11° of sunlight. The ATCA observations of November 1997 were made near western quadrature, so the west limb was in 11° of sunlight. If this is the explanation, then an effect such as the solar radiation or a dawn-dusk electric field must enhance the synchrotron radiation from the limb that is in sunlight. We know of no mechanism to do this. 4) The asymmetry is apparent, with refraction in the Io torus being different for the east and west limbs. We estimate that when $CML = 100°$ and $\lambda_{III} = 190°$ crosses the east limb, the synchrotron radiation from the magnetic equator passes about 0.15 R_J below the center of the Io torus, whose radius is about 1 R_J and whose maximum density, about 10^3 cm^{-3}, varies with longitude. The density gradient in the torus then refracts the radiation southward. Conversely when $CML = 280°$ and the region at $\lambda_{III} = 190°$ crosses the west limb, the radiation passes about 0.15 R_J above the center and at a different longitude in the torus, and the radiation is refracted northward. While the refraction at $\lambda \approx 20$ cm is very small, it may be enough to account for the small asymmetry observed.

3.4. Radius and latitude of the magnetic equator of 1.2 G

In the images at varying CMLs, we have measured the radius and latitude and brightness of the maximum of intensity on both the east and west limbs. For the reasons mentioned above and in

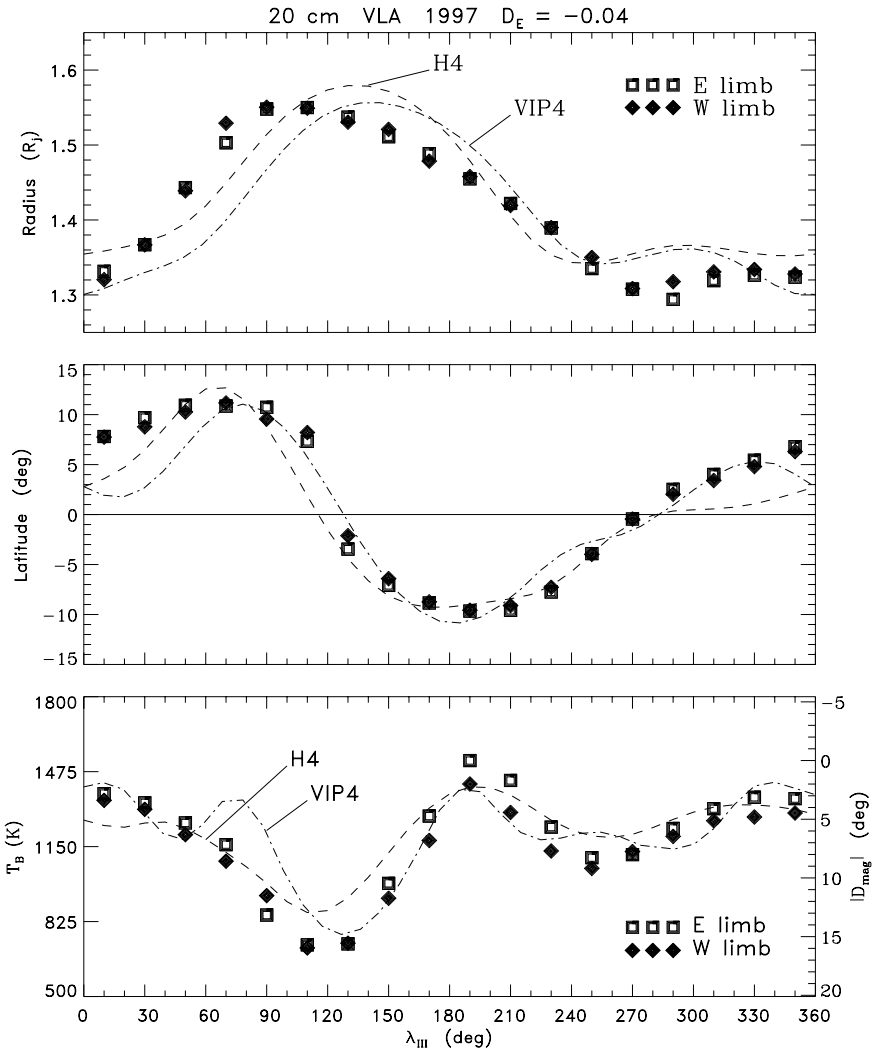

Fig. 4. The symbols show the radius, latitude and maximum brightness temperatures. λ_{III} of the equatorial radiation as observed on the east and west limbs (left scale). The curves calculated from the VIP4 and H4 models show the radius, latitude and $|D_{mag}|$ (right scale) of the magnetic equator of $B = 1.2$ G.

Paper I, we consider that the radius and latitude of these maxima lie on the warped magnetic equator, and that they follow a locus of constant B of approximately 1.2 G.

Fig. 4 shows the radius, latitude and brightness temperature of the east and west limb intensity maxima as observed at the VLA in May 1997 when D_E was near zero. We have similar observations from the other data sets at $D_E \neq 0°$. In those observations (not shown here) the variations with λ_{III} of the radius and latitude are almost identical to the variations in Fig. 4. This is because the locus of maximum intensity is fixed by the field, and is completely independent of D_E.

We see in Fig. 4 that, within the errors, the radius and latitude observed on the two limbs are the same. The variation of radius with λ_{III} is not well matched by calculations from either the H4 or VIP4 models. The difference between observations and models is very similar to that found in the 3-D reconstructions of Paper I, i.e. the increase in radius occurs about 30° earlier than in the models, and the latitude near 0° is higher than in the models.

While the form of the variation of radius with λ_{III} from the imaging here is the same as from the 3-D reconstruction, the values here are about 0.1 R_J smaller. The reason for the difference is that images are biased (Dulk et al. 1997). For high resolution images, the bias is inwards because the radiation belt is, approximately, a torus and so there is a contribution to the brightness from the parts of the torus at smaller projected radii, in front of and behind the plane of the sky. There is not a similar bias in the results from 3-D reconstructions (Sault et al. 1997; Dulk et al. 1999).

A notable feature in the latitude data is the rapid shift from about $+7°$ at $\lambda_{III} = 110°$ to $-3°$ at $\lambda_{III} = 130°$. A similar reduction of the observations with $\pm 10°$ resolution in λ_{III} (here it is $\pm 20°$) confirms and emphasizes the rapid shift. This rapid shift is an artifact resulting from two-dimensional imaging that the 3-D reconstruction avoids. The artifact results from the relatively sharp maximum of D_{mag} at $\lambda_{III} \approx 120°$: the emission seen when $\lambda_{III} = 120°$ traverses a limb is actually from two regions, one north of the equator at λ_{III} somewhat less than 120°, and the other south of the equator at λ_{III} somewhat more that 120°. Thus there is a sudden switch when rotation dictates that the second region beams toward Earth more effectively than the first. This is evident in images on either side of 120°:

the emission has a large north-south extent, with the maximum tending to the south with increasing λ_{III}. When we search for the maximum brightness in the images of limited angular and longitudinal resolution, it shifts rapidly from north to south. It is worth noting that the radius is nearly constant when the latitude shift occurs.

4. Discussion and conclusion

We have considered observations of Jupiter's synchrotron radiation belts over a period of several years while the Earth's declination D_E changed from near its maximum southerly value of $-2.9°$ to near $0°$. We have concentrated on the component of the radiation that outlines the magnetic equator, and particularly on the locus of brightness maxima that follows the magnetic equator corresponding along a fixed value of B of approximately 1.2 G. We have demonstrated that, when D_E is only 1 or 2° away from zero, there is an east-west asymmetry: the brightness of a given location when it traverses the east limb is distinctly different from when it traverses the west limb, 180° of rotation later.

The investigation of this east-west asymmetry and its changes with D_E has led to an understanding of the form of the magnetic equator and its warp as described by the magnetic declination D_{mag}. With the 1995 ATCA data and knowledge of D_{mag}, Dulk et al. (1997) were able to predict that the brightness distribution of the equatorial radiation would change with D_E as found here, and that the east-west asymmetry would tend to zero as D_E approaches zero and then reverse as D_E becomes positive. Similarly the longitude λ_{III} of maximum brightness, which was different by about 30° for the two limbs at $D_E = -2.9°$, was predicted to become the same at $D_E = 0°$ and then to separate in the opposite sense as D_E becomes positive.

Comparisons with models of the magnetic field leave little doubt that the radius, latitude and brightness of the locus of maximum intensity is due to relativistic electrons with pitch angle $\alpha_{\rm eq} \approx 90°$, and its variation with longitude depends entirely, or almost entirely, on the magnetic field of Jupiter, and not on the energy distribution of the relativistic electrons.

At the present time the Earth is moving to the north of Jupiter's rotational equator, so D_E is becoming positive. The east-west asymmetry should reappear, but in the opposite sense, i.e. at most longitudes λ_{III} the brightness at west limb passage will be higher than at east limb passage. For the magnetic equatorial component of synchrotron radiation, it is now understandable why, according to an oft-quoted dictum, "With Jupiter, D_E explains all".

Acknowledgements. The Australia Telescope is funded by the Commonwealth of Australia for operation as a National Facility managed by CSIRO. The National Radio Astronomy Observatory is a facility of the National Science Foundation operated under cooperative agreement by Associated Universities Inc. RJS acknowledges a grant from the Australia-France Cooperative Program. GAD and YL acknowledge grants from the French National Program for Planetology.

References

Dulk, G.A., Leblanc, Y., Sault, R.J., Ladreiter, H.P., Connerney, J.E., 1997, Astron. Astrophys., 319, 282

Dulk, G.A., Leblanc, Y., Sault, R.J., Bolton, S.J., Connerney, J.E.C., 1999, Astron. Astrophys., this issue (Paper I)

Leblanc, Y., Dulk, G.A., Sault, R.J., Hunstead, R.W., 1997, Astron. Astrophys., 319, 274

Sault, R.J., Oosterloo, T., Dulk, G.A., Leblanc, Y., 1997, Astron. Astrophys., 324, 1190